Laser filaments generated and transmitted in highly turbulent air

R. Ackermann, G. Méjean, J. Kasparian, J. Yu, E. Salmon, and J.-P. Wolf

Laboratoire de Spectrométrie Ionic et Moléculaire, Unité Mixte de Recherche Associée au Centre National de la Recherche Scientifique 5579, Université Claude Bernard Lyon 1, 43 bd du 11 Novembre 1918, F-69622 Villeurbanne Cedex, France

Received July 28, 2005; accepted July 28, 2005

The initiation and propagation of a filament generated by ultrashort laser pulses in turbulent air is investigated experimentally. A filament can be generated and propagated even after the beam has propagated through strongly turbulent regions, with structure parameters C_n^2 as many as 5 orders of magnitude larger than those encountered in the usual atmospheric conditions. Moreover, the filament's position within the beam is not affected by the interaction with a turbulent region. This remarkable stability is allowed by the strong Kerr refractive-index gradients generated within the filament, which exceed the turbulence-induced refractive-index gradients by 2 orders of magnitude. © 2006 Optical Society of America

OCIS codes: 010.7060, 010.3310, 190.5940, 190.3270, 190.7110.

High-power, ultrashort (femtosecond) laser pulses can propagate in air in a strongly nonlinear mode; such propagation is referred to as filamentation[1] if the beam reaches a critical power [e.g., $P_{cr}=3.37\,\lambda^2/(8\pi n_2)$ for Gaussian beams, i.e., $P_{cr}=3$ GW in air at 800 nm, with $n_2=3\times10^{-23}$ m^2/W], allowing Kerr-lens self-focusing to overcome diffraction. Then a dynamic balance[2,3] between the Kerr effect and the defocusing on the plasma generated by multiphoton ionization[4,5] in air results in one or several filaments with diameter $d\sim100$ μm. Although the Rayleigh length for such a diameter is only 4 cm, the filamentation can be observed over many tens of meters[6] and generated at several kilometers' distance.[7] Their high intensity [$\sim10^{14}$ W/cm^2; Ref. 8] permits efficient self-phase modulation and generation of a broadband white-light continuum spanning the ultraviolet[9] to the mid infrared.[10]

These properties open exciting prospects for atmospheric applications.[11] The broad supercontinuum facilitates nonlinear and multispectral lidar remote sensing for detection of multiple pollutants and identification of aerosols.[12] The plasma channels generated in the filaments are suitable for high-voltage discharge switching and guiding, opening prospects for lightning control.[13,14] Finally, the possibility of remotely delivering high intensities permits remote elemental analysis.[15] Open-field applications in turn stimulate the need for better knowledge of filament propagation in perturbed atmospheres.

Recent results, both experimental[16] and theoretical,[17] have shown that filaments can survive their interaction with aerosols. Yet, in dry atmospheres, the main optical perturbation is turbulence, which strongly affects beam profiles and pointing stabilities. The effect of turbulence on the filaments and their pointing stability has been observed and modeled in air[18,19] and in water[20] by several groups of scientists, but no comprehensive data sets to characterize the effect of turbulence in various conditions have been reported. In this Letter we characterize the threshold of the structure parameter for the refractive index, C_n^2, for which filamentation in air can occur and survive, depending on the position of the perturbation relative to the filament's onset. C_n^2 is defined from the Kolmogorov theory for turbulence as

$$C_n^2(r)=\frac{\langle[n(r)-n(r+\Delta r)]^2\rangle}{\Delta r^{2/3}},\qquad(1)$$

where r is the location of the perturbation and separation Δr is a length scale within the inertial range, i.e., a few millimeters in typical atmospheric conditions near the ground.[21]

In our experiments (Fig. 1), a chirped-pulse amplification Ti:sapphire laser system delivered 300 fs pulses of 8 mJ energy at a 22.5 Hz repetition rate, centered at 810 nm, with ~10 mm beam diameter (at $1/e^2$ level). The beam was focused by a spherical mirror with 5 m focal length. The origin for the propagation axis ($z=0$) was taken at the nonlinear focus (filament onset, ~2.5 m downstream of the spherical mirror). The filament length was ~2 m. At a given position z, the beam crossed a perpendicular hot air flow (up to 500°C and 500 l/min flow at 20 m/s at the exit port, with a divergence of 20° full angle). Varying distance d between the air blower and the beam from 1 mm to 2 m permitted us to reach C_n^2 values up to 10^{-8} m$^{-2/3}$, as monitored by use of the pointing stability of an elastically transmitted low-power laser. Pointing stabilities were characterized on series of 50 pictures on a screen ($z=7.6$ m) of the lasers transmitted through the turbulent region. The images were

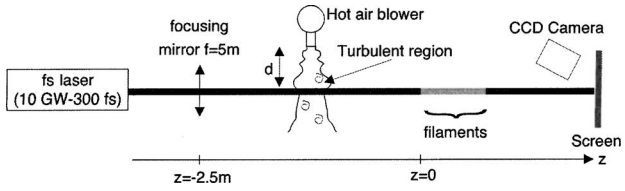

Fig. 1. Experimental setup.

0146-9592/06/010086-3/$0.00

Table 1. Standard Deviation (μrad^2) of the Beam Pointing and of the Filament Position Relative to the Beam on a Screen at $z=2.6$ m.

Title	Unperturbed Beam	Turbulence ($C_n^2=6\times10^{-10}$ m$^{-2/3}$ at $z=1$)
Whole beam pointing	351	856
Filament position relative to the beam	243	224

recorded by a (RGB) red–green–blue CCD camera (10.6 μm/pixel resolution, i.e., typically 10 μrad on the laser beam deflection) equipped with an RG780 colored glass filter to block the fundamental wavelength. First we investigated possible beam stabilization by nonlinear propagation by comparing the pointing stability in the same turbulence conditions of three laser beams: (i) the filamenting beam; (ii) the same ultrashort, infrared laser at a reduced power below filamentation threshold (~1 mJ, i.e., 3 GW peak power); and (iii) a cw 10 mW He–Ne laser beam. We defined the beam position as the center of gravity of the region within the beam profile where the intensity was more than 70% of the maximum on the red layer of the images. The resulting accuracy of a few pixels was comparable to the unperturbed beam-pointing stability. Then the variances σ_x^2 and σ_y^2 in both the x and y positions of the beam yield the average C_n^2 structure parameter for the refractive index through the relation[22]

$$C_n^2 = \sigma^2 \phi^{1/3}/(2.91l), \tag{2}$$

where ϕ is the beam diameter and l is the length of the turbulent path. Here σ^2 ($\sigma^2=\sigma_x^2$, σ_y^2) is expressed in squared radians and C_n^2 is in units of m$^{-2/3}$. The factor of 2.91 is derived for plane waves, and applies with a good approximation to the beams used in these experiments. The three laser configurations had the same pointing stability for identical perturbations. Therefore nonlinear propagation does not improve the pointing stability of the overall beam.

We then characterized the stability of the filament itself by installing the screen in the filamenting region ($z=2.6$ m). The screen was continually moved during the acquisitions such that each shot met a new screen region. An unperturbed He–Ne beam shone on the screen served as a reference for the beam's position. The center of the overall beam and the filament's position were located by use of the blue and green layers of the RGB images, respectively. We assessed the beam's position by thresholding a noise-filtered image and then determining the center of gravity of the beam's contour. Whereas the turbulence generates random shot-to-shot pointing fluctuations of the overall beam, the pointing stability of the filament relative to the beam is unaffected by the perturbation located both at the onset of filamentation ($z=0$) and in the filament ($z=1$; Table 1). This stabilization raises the hope that beam profiles can be transmitted nonlinearly with reduced blur through turbulent regions and could, e.g., permit spatial multiplexing in open-space laser telecommunications. It may have contributed to the beam-profile memory effect observed after several kilometers' vertical propagation.[7]

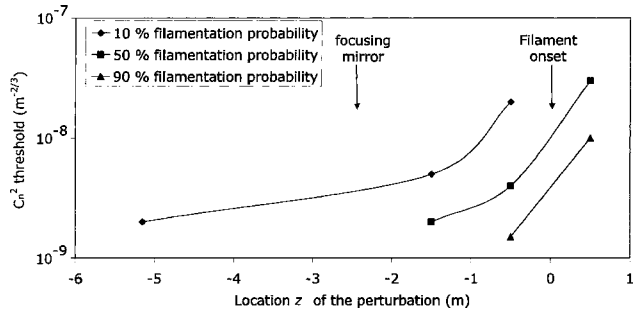

Fig. 2. C_n^2 threshold for 90%, 50%, and 10% probability of generating a filament as a function of location z of the turbulent region.

However, a key feature for atmospheric applications is the ability of the filaments to survive their propagation through turbulence. We characterized the occurrence of a filament in given conditions by setting a threshold value on the integrated contribution of the green layer of the recorded RGB beam profiles. This automated criterion corresponded well to visual observation of a filament. A statistical analysis based on the binomial law shows that, for 50 pictures in each condition, the confidence interval for the rate of filament occurrence is limited to ±10% in the worst case (50% occurrence rate). Therefore the observed changes in filament occurrence rates are statistically significant. The C_n^2 parameter was monitored by use of the main laser beam ($\phi=10$ mm) on the same records. This procedure limits the influence of fluctuations and drifts, knowledge of which is crucial to the study of turbulence, which is a stochastic phenomenon.

The influence of turbulence on the probability of filamentation is found to decrease steeply near nonlinear focus (Fig. 2). Although a moderate perturbation at the exit of the laser can significantly hinder the formation of a filament 5 m downstream, a filament once formed needs a considerable perturbation to be destroyed. Moreover, the C_n^2 values that permit a 90% probability of occurrence of a filament are orders of magnitude greater than any real atmospheric condition [10^{-15} to 10^{-13} m$^{-2/3}$ (Ref. 22]. Although atmospheric applications of filaments require much longer length scales than in our experiments, and although the scaling of laboratory results for strongly nonlinear processes such as turbulence and filamentation are not straightforward, our results suggest that turbulence should not be the limiting factor for applications that require propagation of filaments

across the atmosphere. The high turbulence threshold for filamentation also opens the way to specific applications that may require propagating filaments through highly turbulent regions. Such applications include the new filament-based laser-induced breakdown spectroscopy technique,[15] in the context of combustion metrology, implying highly turbulent fluid flows.[23]

The small effect of turbulence on an already formed filament highlights the intrinsic stability of the filament structure, which can also withstand the interaction with large obscurants[16,17]: In a filament, the phase perturbations induced by the turbulence may be smoothed out. Moreover, we can compare the refractive-index gradients induced by both turbulence, $\nabla n_T \approx 9.1\times10^{-5}\times T_s/(T\Delta r)$, and filamentation, $\nabla n_{\mathrm{fil}} \approx n_2 I/d$, where $I=10^{14}$ W/cm^2 is the typical intensity within the filament, $d\sim100$ μm is the filament's diameter, $T_s=288.15$ K is the standard temperature, T is the temperature, and Δr is the scale of the temperature gradients within the hot air beam. The dimensionless 9.1×10^{-5} factor stems from the Rank formula evaluated at 800 nm.[24] Considering $T=500^\circ$C as an upper bound for the temperature at the exhaust of the hot air blower and estimating that $\Delta r\sim1$ cm, we get $\nabla n_T \approx 6\times10^{-3} m^{-1} \ll \nabla n_{\mathrm{fil}} \approx 0.3$ m^{-1} such that, even for strong structure parameter values, the contribution of turbulence to the refractive-index gradient is negligible compared with that induced by the Kerr effect within the filament. Note that, when lasers are propagated over large distances in the atmosphere, the air pressure varies to a large extent. However, because the distances involved are large, the corresponding index gradients are negligible.

In contrast, an early perturbation in the beam profile will develop further during subsequent propagation because of its nonlinearity and will give rise to turbulent cells within the beam profile, each one generating one or several local intensity maxima. These turbulent cells propagate almost independently of one another.[25] Therefore they can generate filaments only if they contain several critical powers. If they are too small, filamentation will be impossible.

In conclusion, we have shown that filamentation is not affected by turbulence in the ranges that can be encountered in the atmosphere. For stronger turbulence, filamentation may be stopped or prevented, with a relatively sharp cutoff of the filamentation when turbulence increases. The effect of the perturbation is greater when the turbulent region is located at the early stages of propagation of the laser beam.

We acknowledge helpful discussions with Matthieu Jomier about the image analysis. J. Kasparian's e-mail address is jkaspari@lasim-univ-lyon1.fr.

References

1. A. Braun, G. Korn, X. Liu, D. Du, J. Squier, and G. Mourou, Opt. Lett. **20**, 73 (1995).
2. A. Brodeur, C. Y. Chien, F. A. Ilkov, S. L. Chin, O. G. Kosareva, and V. P. Kandidov, Opt. Lett. **22**, 304 (1997).
3. M. Mlejnek, E. M. Wright, and J. V. Moloney, Opt. Lett. **23**, 382 (1998).
4. H. Schillinger and R. Sauerbrey, Appl. Phys. B **68**, 753 (1999).
5. J. Kasparian, R. Sauerbrey, and S. L. Chin, Appl. Phys. B **71**, 877 (2000).
6. B. La Fontaine, F. Vidal, Z. Jiang, C. Y. Chien, D. Comtois, A. Desparois, T. W. Johnston, J.-C. Kieffer, H. Pépin, and H. P. Mercure, Phys. Plasmas **6**, 1615 (1999)
7. M. Rodriguez, R. Bourayou, G. Méjean, J. Kasparian, J. Yu, E. Salmon, A. Scholz, B. Stecklum, J. Eislöffel, U. Laux, A. P. Hatzes, R. Sauerbrey, L. Wöste, and J.-P. Wolf, Phys. Rev. E **69**, 036607 (2004).
8. A. Becker, N. Aközbek, K. Vijayalakshmi, E. Oral, C. M. Bowden, and S. L. Chin, Appl. Phys. B **73**, 287 (2001).
9. N. Aközbek, A. Iwasaki, A. Becker, M. Scalora, S. L. Chin, and C. M. Bowden, Phys. Rev. Lett. **89**, 143901 (2002).
10. J. Kasparian, R. Sauerbrey, D. Mondelain, S. Niedermeier, J. Yu, J.-P. Wolf, Y.-B. André, M. Franco, B. Prade, A. Mysyrowicz, S. Tzortzakis, M. Rodriguez, H. Wille, and L. Wöste, Opt. Lett. **25**, 1397 (2000).
11. J. Kasparian, M. Rodriguez, G. Méjean, J. Yu, E. Salmon, H. Wille, R. Bourayou, S. Frey, Y.-B. André, A. Mysyrowicz, R. Sauerbrey, J.-P. Wolf, and L. Wöste, Science **301**, 61 (2003).
12. G. Méjean, J. Kasparian, J. Yu, S. Frey, E. Salmon, and J.-P. Wolf, Appl. Phys. B **78**, 535 (2004).
13. B. La Fontaine, D. Comptois, C. Y. Chien, A. Desparois, F. Gérin, G. Jarry, T. W. Johnston, J. C. Kieffer, F. Martin, R. Mawassi, H. Pépin, F. A. M. Rizk, F. Vidal, C. Potvin, P. Couture, and H. P. Mercure, J. Appl. Phys. **88**, 610 (2000).
14. R. Ackermann, K. Stelmaszczyk, P. Rohwetter, G. Méjean, E. Salmon, J. Yu, J. Kasparian, G. Méchain, V. Bergmann, S. Schaper, B. Weise, T. Kumm, K. Rethmeier, W. Kalkner, J. P. Wolf, and L. Wöste, Appl. Phys. Lett. **85**, 5781 (2004).
15. K. Stelmaszczyk, P. Rohwetter, G. Méjean, J. Yu, E. Salmon, J. Kasparian, R. Ackermann, J.-P. Wolf, and L. Wöste, Appl. Phys. Lett. **85**, 3977 (2004).
16. F. Courvoisier, V. Boutou, J. Kasparian, E. Salmon, G. Méjean, J. Yu, and J.-P. Wolf, Appl. Phys. Lett. **83**, 213 (2003).
17. M. Kolesik and J. V. Moloney, Opt. Lett. **29**, 590 (2004).
18. V. P. Kandidov, O. G. Losareva, E. I. Mozhaev, and M. P. Tamarov, Atmos. Ocean. Opt. **13**, 394 (2000).
19. S. L. Chin, A. Talebpour, J. Yang, S. Petit, V. P. Kandidov, O. G. Kosareva, and M. P. Tamarov, Appl. Phys. B **74**, 67 (2002).
20. W. Liu, O. Kosareva, I. S. Golubtsov, A. Iwasaki, A. Becker, V. P. Kandidov, and S. L. Chin, Appl. Phys. B **75**, 595 (2002).
21. V. I. Tatarskii, *The Effects of the Turbulent Atmosphere on Wave Propagation* (Keter, Jerusalem, 1971).
22. S. Bendersky, N. S. Komeika, and N. Blaunstein, Appl. Opt. **43**, 4070 (2004).
23. V. Sturm and R. Noll, Appl. Opt. **42**, 6221 (2003).
24. D. H. Rank, in *Advances in Spectroscopy I*, H. W. Thompson, ed. (Interscience, 1959), Chap. 10.
25. M. Mlejnek, M. Kolesik, E. M. Wright, and J. V. Moloney, Phys. Rev. Lett. **83**, 76 (1999).